Indirect Rotor Field-Oriented Control of Fault-Tolerant Drive System for Three-Phase Induction Motor with Rotor Resistance Estimation Using EKF

M. Jannati*, N. R. N. Idris, M. J. A. Aziz
Universiti Teknologi Malaysia, UTM-PROTON Future Drive Laboratory, Faculty of Electrical Engineering,
81310 Skudai, Johor Bahru, MALAYSIA
*Corresponding author, e-mail: Jannatim94@yahoo.com

Abstract

The performance of an Indirect Rotor Field-Oriented Control (IRFOC) scheme for Induction Motors (IMs) is strongly dependent on the motor parameters especially, rotor resistance. As such, to ensure high performance drive system, the variation of the rotor resistance due to the temperature increase need to be estimated based on the available terminal variables. However, the algorithm used to estimate the rotor resistance for a balanced Three-Phase Induction Motor (TPIM) cannot be used for an open-phase fault IM; this is because the model of a faulty machine is different from the balanced 3-phase machine. In this paper, an IRFOC of fault-tolerant drive system (with stator open-phase fault) for a TPIM with rotor resistance estimation using Extended Kalman Filter (EKF) is proposed. The performance of the EKF based rotor resistance estimator is evaluated under different operating conditions using MATLAB simulation package. The proposed algorithm for estimation of rotor resistance in this paper can be applied to either balanced TPIM or Faulty TPIM (FTPIM). The simulation results showed that the proposed system is able to overcome the rotor resistance variations, load disturbance as well as stator open-phase fault condition, with good tracking capability.

Keywords: TPIM, IRFOC, EKF, rotor resistance estimation, fault-tolerant drive system, simulation

1. Introduction

In some applications, such as in military, space exploration and electric vehicle, Faulty Three-Phase Induction Motor (FTPIM) control is very significant and vital (in this paper, FTPIM is referred to stator open-phase fault). For safety reasons, these applications require a fault-tolerant control method whereby the drive system operation cannot be stopped even under faulty condition. In these situations, the drive system should keep its minimum operating performance at least until the fault is rectified. It is well known that the most widely adopted control for electrical machines is the Field-Oriented Control (FOC) or vector control [1-4]. In order to ensure continuous operation of FOC under faulty conditions, the algorithm must be modified to cater for the unbalance faulty conditions. If a conventional vector control technique is applied to an open-phase faulty induction machine, severe oscillations in the torque, and hence the speed may be observed [5, 6]. Several researches have been conducted to study on the faulty IM and hence modifications needed to be applied to the conventional vector control scheme under faulty conditions. A fault-tolerant drive system for Indirect Rotor FOC (IRFOC) of TPIM based on rotational transformations was proposed in [5, 6]; it was shown that by using some minor modification to the conventional IRFOC for TPIM, the FOC of unbalanced or FTPIM is possible.

In IRFOC, an accurate estimation of rotor resistance, regardless of whether the machine is a balanced TPIM or FTPIM, is vital to ensure high performance torque control [7]. In this paper, focus is given to the problem of parameter variation (i.e. rotor resistance, r_r) of the induction machine under faulty conditions (one phase cut-off). Inaccurate value of rotor time constant ($T_r=L_r/r_r$; where L_r is the stator inductance) used in FOC algorithm will result in an improper decoupled between torque and flux components [8]. In practice, the value of r_r increases with temperature after operating the motor over a certain period of time. It was reported that the r_r can vary to as high as 100% of its nominal value [9-11]. The variation of r_r

from its nominal value (hence the variation in T_r) can significantly affect the performance of the IRFOC especially for TPIM under fault condition. Therefore in order to maintain the highest performance of IRFOC, estimation of rotor resistance under faulty condition is mandatory.

One of the most effective algorithms used in the estimation of parameters, such as speed and resistance, for electrical machines is the Extended Kalman Filter (EKF) [12-14]. EKF is a type of observer that considers the nonlinearity of the machine model, filters the measured noises and system noises, and estimates the states variables [13]; this is the reason why the EKF has established extensive applications in control systems. In this work, a robust IRFOC method for a fault-tolerant drive system based on EKF is proposed. At the same time, another EKF is also used to estimate the rotor resistance for IRFOC scheme. In this paper, simulation results obtained for a fault-tolerant drive system based on IRFOC, with and without rotor resistance estimation are presented. The dynamics and the performance characteristics of the proposed method are verified and evaluated using MATLAB software.

The rest of the paper is organized as follows: In section 2, the d-q model of FTPIM is presented. The IRFOC equations for a fault-tolerant drive system as well as the structure of the proposed technique are presented in section 3. EKF equations for rotor resistance estimation for fault-tolerant drive system are given in section 4. In section 5, the results are presented and discussed and finally section 6 concludes the paper.

2. d-q Model of FTPIM

As mentioned earlier, the fault condition assumed in this paper is a phase cut-off. Specifically, it will be assumed that a phase cut-off fault occurred in phase "c" of a TPIM. With this faulty condition, the electrical equations with symmetrical stator windings in a stationary reference (superscript "s") can be described by Equation (1)-(9) [5].

$$v_{ds}^s = r_s i_{ds}^s + \frac{d\lambda_{ds}^s}{dt} \tag{1}$$

$$v_{qs}^s = r_s i_{qs}^s + \frac{d\lambda_{qs}^s}{dt} \tag{2}$$

$$\lambda_{ds}^s = L_{ds} i_{ds}^s + M_d i_{dr}^s \tag{3}$$

$$\lambda_{qs}^s = L_{qs} i_{qs}^s + M_q i_{qr}^s \tag{4}$$

$$0 = r_r i_{dr}^s + \frac{d\lambda_{dr}^s}{dt} + \omega_r \lambda_{qr}^s \tag{5}$$

$$0 = r_r i_{qr}^s + \frac{d\lambda_{qr}^s}{dt} - \omega_r \lambda_{dr}^s \tag{6}$$

$$\lambda_{dr}^s = M_d i_{ds}^s + L_r i_{dr}^s \tag{7}$$

$$\lambda_{qr}^s = M_q i_{qs}^s + L_r i_{qr}^s \tag{8}$$

Where,

$$L_{ds} = L_{ls} + L_{md}, L_{qs} = L_{ls} + L_{mq}, L_{md} = \frac{3}{2} L_{ms}, L_{mq} = \frac{1}{2} L_{ms}, M_d = \frac{3}{2} L_{ms}, M_q = \frac{\sqrt{3}}{2} L_{ms} \tag{9}$$

In (1)-(9), v_{ds}^s, v_{qs}^s are the stator d-q axes voltages i_{ds}^s, i_{qs}^s are the stator d-q axes currents i_{dr}^s, i_{qr}^s are the rotor d-q axes currents λ_{ds}^s, λ_{qs}^s are the stator d-q axes fluxes and λ_{dr}^s and λ_{qr}^s are the rotor d-q axes fluxes in the stator reference frame. r_s and r_r are the stator and rotor resistances, respectively. L_{ds}, L_{qs}, L_r, M_d and M_q denote the stator, the rotor self and mutual

inductances. ω_r is the motor speed. Electromagnetic torque and mechanical equations can be written as follows:

$$\tau_e = \frac{P}{2}(M_q i_{qs}^s i_{dr}^s - M_d i_{ds}^s i_{qr}^s)$$
(10)

$$\tau_e - \tau_l = \frac{2}{P}\left(J\frac{d\omega_r}{dt} + F\omega_r\right)$$
(11)

In (10) and (11), τ_e and τ_l are electromagnetic torque and load torque and P, J and F are the number of poles, moment of inertia and viscous friction coefficient respectively. As can be seen from (1)-(11), the equations of FTPIM are similar to the balanced one. In fact, by substituting $M_d=M_q=M=3/2L_{ms}$ and $L_{ds}=L_{qs}=L_s=L_{ls}+3/2L_{ms}$ in the FTPIM equations, we can obtain the familiar equation of TPIM. Because of the asymmetrical structure of FTPIM, conventional vector control algorithm for symmetrical IM cannot be directly used for controlling the FTPIM since it will result in a significant ripple in the torque and speed [5, 6]. To overcome this problem, similar method as introduced in [5] will be used here. In [5], two rotational transformations for variables transformation from unbalanced set (e.g., FTPIM) to the balanced set (e.g., TPIM) have been proposed. These rotational transformations are given by (12) and (13).

$$\begin{bmatrix} i_{ds}^e \\ i_{qs}^e \end{bmatrix} = \begin{bmatrix} T_{is}^e \end{bmatrix}\begin{bmatrix} i_{ds}^s \\ i_{qs}^s \end{bmatrix} = \begin{bmatrix} \dfrac{M_d}{M_q}\cos\theta_e & \sin\theta_e \\ -\dfrac{M_d}{M_q}\sin\theta_e & \cos\theta_e \end{bmatrix}\begin{bmatrix} i_{ds}^s \\ i_{qs}^s \end{bmatrix}$$
(12)

$$\begin{bmatrix} v_{ds}^e \\ v_{qs}^e \end{bmatrix} = \begin{bmatrix} T_{vs}^e \end{bmatrix}\begin{bmatrix} v_{ds}^s \\ v_{qs}^s \end{bmatrix} = \begin{bmatrix} \dfrac{M_q}{M_d}\cos\theta_e & \sin\theta_e \\ \dfrac{M_q}{M_d}\sin\theta_e & \cos\theta_e \end{bmatrix}\begin{bmatrix} v_{ds}^s \\ v_{qs}^s \end{bmatrix}$$
(13)

Where, θ_e is the angle between the stationary reference frame and the rotor field-oriented reference frame. It can be shown that by applying these transformations, the asymmetric equations of the FTPIM become similar to the structure of equations for the balanced TPIM [5]. With some minor changes in the TPIM parameters, it is possible to apply the conventional IRFOC method to the FTPIM [5].

3. Fault-tolerant Drive System Based on IRFOC
Open circuit fault is one of most familiar failures in the IMs stator windings [15-18]. In the literature, different methods have been proposed to detect stator and rotor faults in electrical machines [15-18]. These techniques provide approximately immediate open stator winding detection and will be assumed in this paper.
The objective of FOC is to separate the motor currents into flux and torque producing components. The torque is proportional to the product of these two components and they can be treated separately. In RFOC method, the rotor flux vector is aligned with d-axis ($\lambda_{dr}^e=|\lambda_r|$, $\lambda_{qr}^e=0$) [8]. With this assumption and by applying (12) and (13) to the equations of FTPIM (equations (1)-(11)) and by considering of $L_{ds}/L_{qs}=(M_d/M_q)^2$, (in the FTPIM: $M_d=3/2L_{ms}, M_q=\sqrt{3}/2L_{ms}, L_{ds}=L_{ls}+1/2L_{ms}$, $L_{qs}=L_{ls}+1/2L_{ms}$ and $L_{ms}>>L_{ls}$), RFOC equations for FTPIM are obtained as following equations:

$$|\lambda_r| = \frac{M_q i_{ds}^e}{1 + T_r d/dt} \quad , \quad \omega_e = \omega_r + \frac{M_q i_{qs}^e}{T_r |\lambda_r|} \quad , \quad \tau_e = \frac{P}{2} \frac{M_q}{L_r} |\lambda_r| i_{qs}^e \tag{14}$$

$$v_{ds}^e = v_{ds}^d + v_{ds}^{ref} + v_{ds}^{-e} \tag{15}$$

$$v_{qs}^e = v_{qs}^d + v_{qs}^{ref} + v_{qs}^{-e} \tag{16}$$

Where,

$$v_{ds}^d = -\omega_e i_{qs}^e (L_{qs} - \frac{M_q^2}{L_r}) + (\frac{M_q}{L_r})(\frac{M_q i_{ds}^e - |\lambda_r|}{T_r}) \tag{17}$$

$$v_{qs}^d = \omega_e i_{ds}^e (L_{qs} - \frac{M_q^2}{L_r}) + \omega_e M_q \frac{|\lambda_r|}{L_r} \tag{18}$$

$$v_{ds}^{ref} = (\frac{r_s M_q^2 + r_s M_d^2}{2M_d^2}) i_{ds}^e + (L_{qs} - \frac{M_q^2}{I_r}) \frac{di_{ds}^e}{dt} \tag{19}$$

$$v_{qs}^{ref} = (\frac{r_s M_q^2 + r_s M_d^2}{2M_d^2}) i_{qs}^e + (L_{qs} - \frac{M_q^2}{I_r}) \frac{di_{qs}^e}{dt} \tag{20}$$

$$v_{ds}^{-e} = \left(\frac{r_s M_q^2 - r_s M_d^2}{2M_d^2} \right) \left(\cos 2\theta_e i_{ds}^e - \sin 2\theta_e i_{qs}^e \right) \tag{21}$$

$$v_{qs}^{-e} = \left(\frac{r_s M_q^2 - r_s M_d^2}{2M_d^2} \right) \left(-\sin 2\theta_e i_{ds}^e - \cos 2\theta_e i_{qs}^e \right) \tag{22}$$

The superscript "e" indicates the variables are in the rotating reference frame. Moreover, T_r and ω_e are rotor time constant ($T_r = L_r/r_r$) and the angular velocity of the RFO reference frame respectively. As shown by using these rotational transformations (equations (12) and (13)), IRFOC equations for FTPIM resemble the IRFOC for balanced TPIM equations. Based on (14)-(22), it can be seen that the only difference between these equations and balanced TPIM equations is that for balanced TPIM, we have r_s, $M=3/2L_{ms}$ and $L_s=L_{ls}+3/2L_{ms}$ [8], but for FTPIM $r_s = (r_s M_q^2 + r_s M_d^2)/2M_d^2$, $M=M_q=\sqrt{3}/2L_{ms}$, $L_s=L_{qs}=L_{ls}+1/2L_{ms}$ and v_{ds}^{-e}, v_{qs}^{-e} as shown in (14)-(22). Therefore, with some minor changes to the parameters of motor, it is possible to apply the conventional IRFOC method to the FTPIM [5, 6].

4. EKF for Rotor Resistance Estimation in Fault-tolerant Drive System

As mentioned before, the performance of the IRFOC depends mainly on the rotor resistance that increases with temperature. In IRFOC, any changes in rotor resistance gives wrong value of rotor time constant and consequently produces error in the estimated rotor flux position. Subsequently, errors in the rotor flux position mean that the decoupling of the torque and flux components of the stator current is compromised and the instantaneous torque response is no longer established. Therefore, online estimation of rotor resistance has to be incorporated in order to improve the performance of the drive system over a wide speed range of operation [7], [19-21]. Evidently, the conventional EKF for rotor resistance estimation in

TPIMs cannot be directly employed for FTPIM because of the different models that are used to describe a balanced TPIM and a FTPIM. This aspect of the study is an extension of the authors' previous research presented in Refs. [5, 6] and [22-29]. In this paper, an EKF is proposed to estimate the rotor resistance for both TPIM and FTPIM in associated with IRFOC.

Figure 1 shows the structure of the proposed fault-tolerant drive system based on IRFOC (details of the fault-tolerant drive system in Figure 1 is given in Appendix A and fully discussed in [5]) with the proposed EKF-based rotor resistance estimator. The estimation is performed by the EKF using measured terminal variables, i.e. rotor speed, stator currents and voltages. The estimated value of rotor resistance is then used in the drive system. In this paper an EKF algorithm with two different parameters for estimation of rotor resistance in fault-tolerant drive system is proposed. The changes of these parameters are performed after the fault is detected and by a switch as shown in Figure 1. In the proposed EKF and under balanced condition, $M_d=M_q=3/2L_{ms}$ and $L_{ds}=L_{qs}=L_{ls}+3/2L_{ms}$ are used in the EKF algorithm. When the fault occurs, the values are substituted with, $M_d=3/2L_{ms}$, $M_q=\sqrt{3/2}L_{ms}$, $L_{ds}=L_{ls}+3/2L_{ms}$ and $L_{qs}=L_{ls}+1/2L_{ms}$. In other words, the proposed EKF based rotor resistance estimation can be used for the balanced TPIM as well as for the FTPIM.
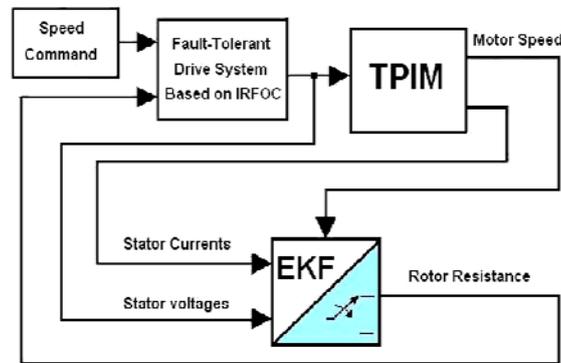
Figure 1. Scheme of Proposed Fault-tolerant Drive System Based on IRFOC

For the purpose of rotor resistance estimation, the d-axis (i_{dr}) and the q-axis (i_{qr}) of the rotor currents as well as the rotor resistance (r_r) are chosen as the state variables. Using these state variables, it is possible to express the state space model of the IM in the form of Equation (23) and (24):

$$\dot{x} = Ax + Bu \tag{23}$$

$$y = Cx \tag{24}$$

In these equations, *A*, *B* and *C* are the system, input and output matrices respectively. *x*, *y* and *u* are the system state matrix, system output matrix and system input matrix respectively. In order to implement and simulate the EKF algorithm, continuous state equations should be transformed into discrete state equations. Therefore, Equation (23) and (24) can be re-written as follows:

$$x(n+1) = \underbrace{(I + Adt)}_{A(n)}x(n) + \underbrace{(Bdt)}_{B(n)}u(n) + w(n) \tag{25}$$

$$y(n) = C(n)x(n) + v(n) \tag{26}$$

Because of IM model accuracy and measurement errors, stochastic variables are introduced (*w*(*n*) is the system noise and *v*(*n*) is the measurement noise). The matrices of *A*(*n*), *B*(*n*) and *C*(*n*) in equations (25) and (26) are given in Appendix B. The matrices *x*(*n*), *y*(*n*) and *u*(*n*) are given as follows:

$$x(n) = \begin{bmatrix} i_{dr}(n) & i_{qr}(n) & r_r(n) \end{bmatrix}^T \tag{27}$$

$$y(n) = \left(\begin{bmatrix} i_{ds}(n) \\ i_{qs}(n) \end{bmatrix} - \begin{bmatrix} 1 - \dfrac{r_s dt}{\sigma_1 L_{ds}} & \dfrac{M_d M_q \omega_r dt}{\sigma_1 L_{ds} L_r} \\ -\dfrac{M_d M_q \omega_r dt}{\sigma_2 L_{qs} L_r} & 1 - \dfrac{r_s dt}{\sigma_2 L_{qs}} \end{bmatrix} \begin{bmatrix} i_{ds}(n\ 1) \\ i_{qs}(n\ 1) \end{bmatrix} - \begin{bmatrix} \dfrac{v_{ds}^s}{\sigma_1 L_{ds}} dt \\ \dfrac{v_{qs}^s}{\sigma_2 L_{qs}} dt \end{bmatrix} \right) \tag{28}$$

$$u(n) = \begin{bmatrix} i_{ds}(n) & i_{qs}(n) & v_{ds}(n) & v_{qs}(n) \end{bmatrix}^T \tag{29}$$

The steps of the EKF algorithm can be formulated as [14]:
 1) Estimation of the Error Covariance Matrix:

$$P(n+1) - \Gamma(n)P(n)\Gamma^T(n) + Q \tag{30}$$

 2) Computation of Kalman Filter Gain:

$$K(n) - P(n+1)\Delta^T(n)\left[\Delta(n)P(n+1)\Delta(n) + R\right]^{-1} \tag{31}$$

 3) Update of the Error Covariance Matrix:

$$P(n) = \begin{bmatrix} 1 & K(n)\Delta(n) \end{bmatrix}P(n\ 1) \tag{32}$$

 4) State Estimation:

$$\hat{x}(n+1) = \hat{x}(n) + K(n)\left[z(n+1) - h(\hat{x}(n+1)) \right] \tag{33}$$

In these equations, Q and R are the covariance matrices of the noises. To begin the calculation, the initial values of the state variables and error covariance matrices (P, Q and R) need to be identified. In this work, the initial values of matrices P, Q and R for estimation of rotor resistance are obtained from the trial and error process.

5. Simulation Results

In order to verify the effectiveness of the proposed structure of IRFOC for fault-tolerant drive system and the EKF based rotor resistance estimation, simulation is conducted using MATLAB simulation package. The parameters that are used for the simulation are given in Appendix C. Three different drive systems are simulated: (1) IRFOC drive without fault-tolerant and without rotor resistance estimator, (2) IRFOC drive with fault-tolerant and without rotor resistance estimator, and (3) IRFOC drive with fault-tolerant and with rotor resistance estimator. The three drive systems are tested under the same operating conditions as follows: a phase cut-off fault is introduced at t=0.5s, the value of the load is increased from zero to 1N.m at t=1.5s (see Figure 2) and the value of the rotor resistance is increased by 100% of its nominal value at t=2s (see Figure 3). In all cases, the reference speed is set to the 500rpm.
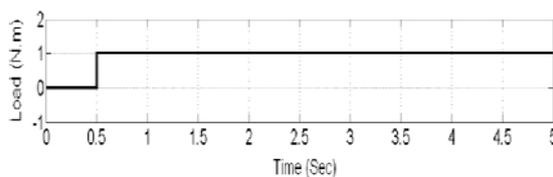
Figure 2. Variation of Load   Figure 3. Variation of Rotor Resistance
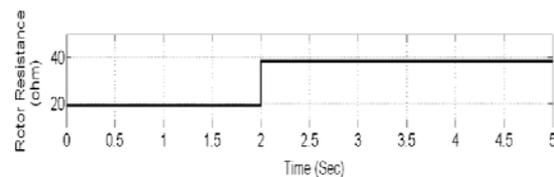
(a) Stator and rotor currents   (b) Speed response

(c) Torque response
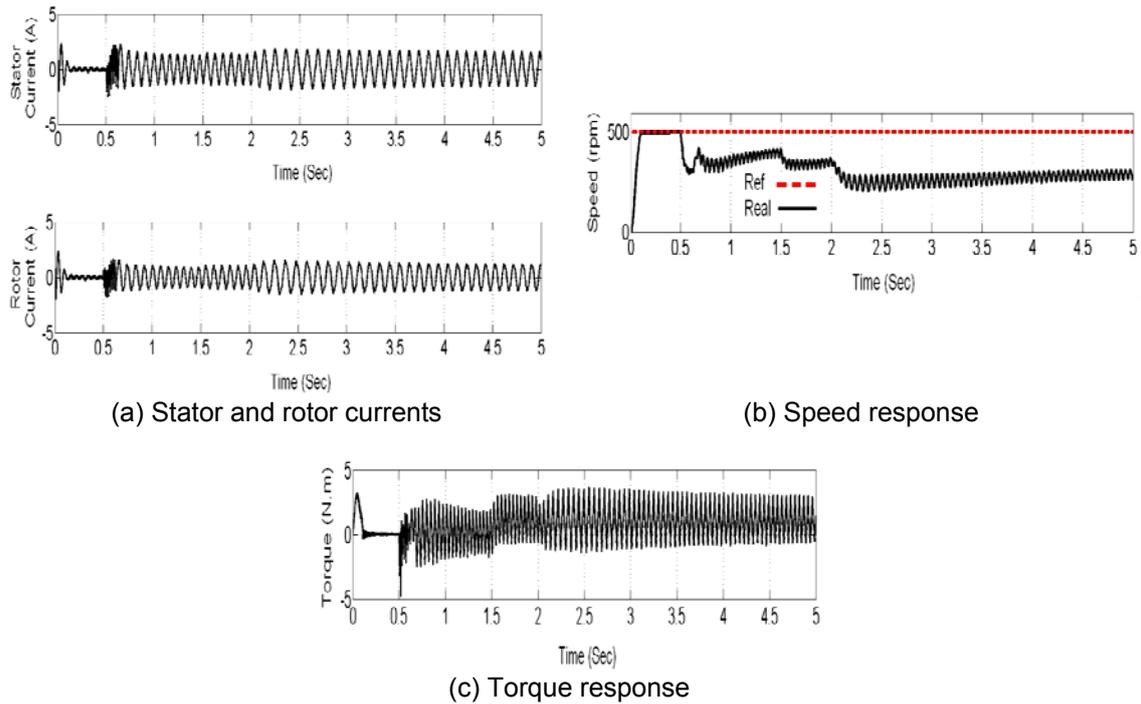
Figure 4. IRFOC Drive without Fault-tolerant and without Rotor Resistance Estimator

(a) Stator and rotor currents   (b) Speed response

(c) Torque response
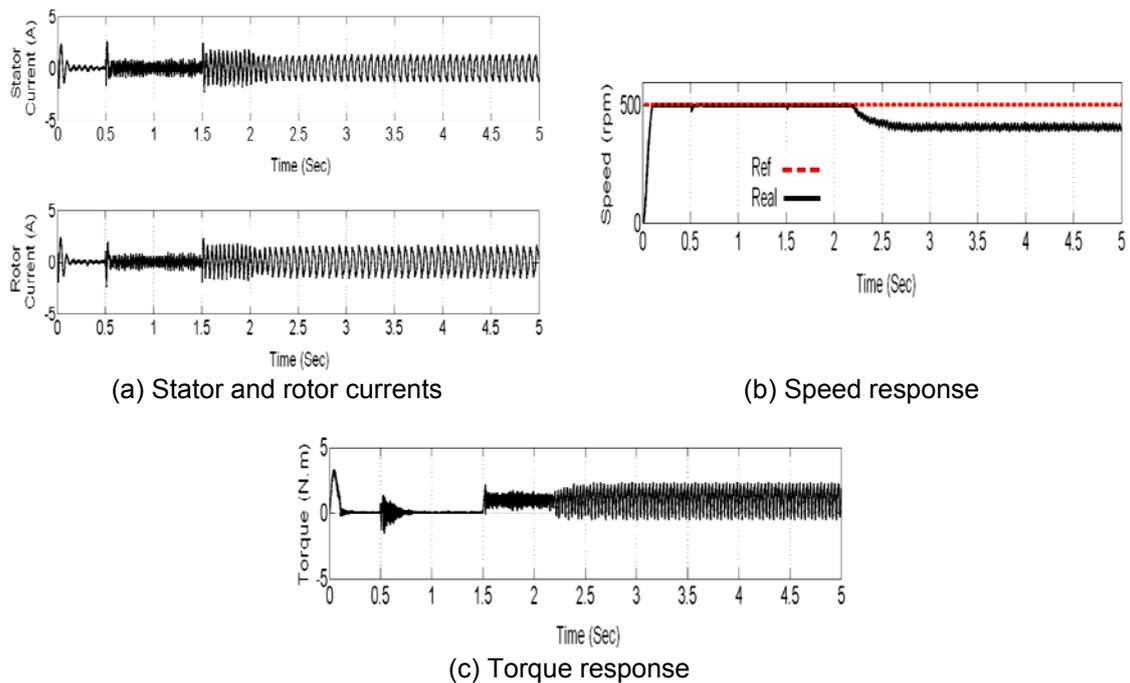
Figure 5. IRFOC Drive with Fault-tolerant and without Rotor Resistance Estimator

(a) Stator and rotor currents

(b) Speed response
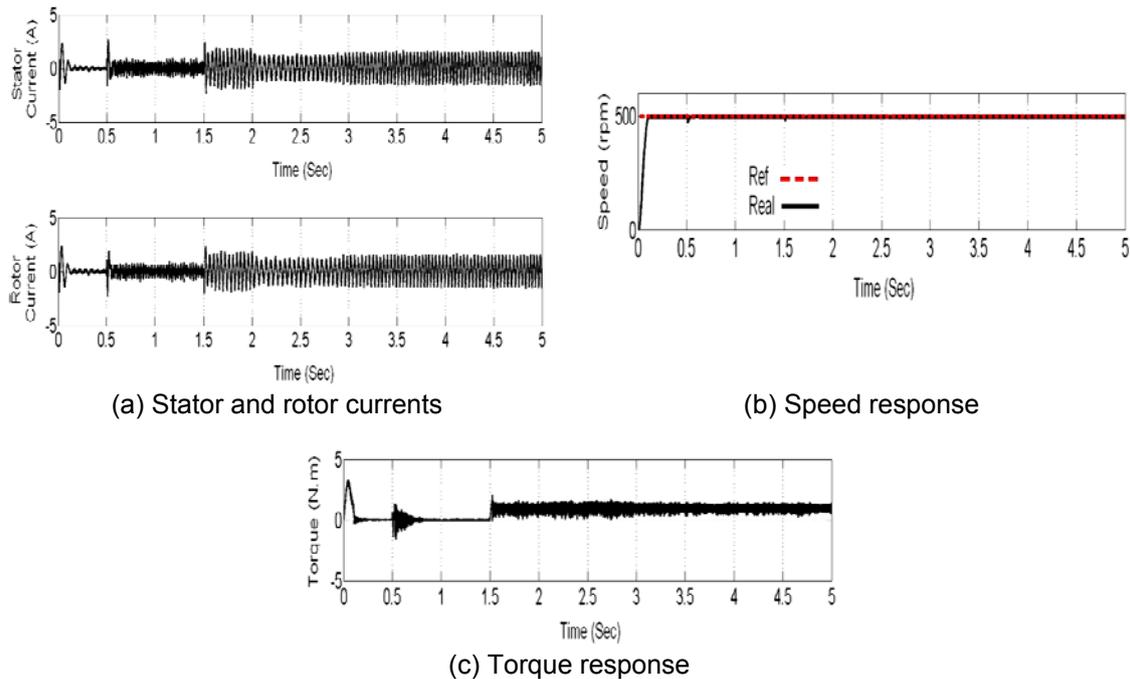
(c) Torque response

Figure 6. IRFOC Drive with Fault-tolerant and with Rotor Resistance Estimator
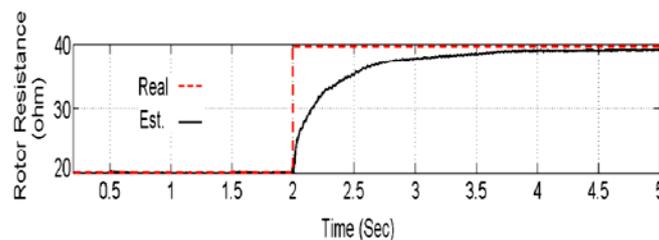
Figure 7. Estimated Rotor Resistance Waveform

The responses of stator and rotor currents, rotor speed and electromagnetic torque of the IRFOC drive systems are shown in Figure 4, Figure 5 and Figure 6, respectively. Without the fault-tolerant drive (Figure 4), severe oscillation in the torque can be seen at the moment the phase cut-off fault is introduced at t=0.5s. The responses are getting worse as the load toque and variation in rotor resistance are introduced at t=1.5s and t=2s, respectively. In Figure 5, where the fault-tolerant is incorporated to the drive system, the phase cut-off faulty can be overcome as soon as the fault-tolerant mechanism is activated (Note: the algorithm used for the fault-tolerant system is fully discussed in [5]). However, as a step change in rotor resistance is introduced at t=2s, the deterioration in the response, particularly the torque response, can be observed. The rotor resistance estimator managed to improve the response by restoring the rotor resistance value used in the control algorithm to the actual value (i.e. twice its nominal value). Figure 6 shows the performance of the estimator in tracking the variation of the rotor resistance. The simulation results demonstrated the robustness of the estimator to a faulty condition the load variations.

6. Conclusion

This paper presents the fault-tolerant drive system for IRFOC with EKF-based rotor resistance estimator. The proposed rotor resistance estimator can be used under normal and phase cut-off condition, with minimal modification to the parameters used in the algorithm.

Simulation results demonstrated the excellence tracking performance of the proposed estimator as well as its robustness against load variation and faulty condition. Since FTPIM and singephase IM can be modelled as unbalanced 3-phase IM, the proposed technique is also applicable to single-phase IMs.

References

[1] H Amimeur, D Aouzellag, R Abdessemed, K Ghedamsi. Sliding mode control of a dual-stator induction generator for wind energy conversion systems. *Int J Electr Power Energy Syst*. 2012; 42(1): 60-70.

[2] A Khedher, M Faouzi Mimouni. Sensorless-adaptive DTC of double star induction motor. *Energy Convers Manage*. 2010; 51(12): 2878-2892.

[3] D Jang. Problems Incurred in Vector Controlled Single-phase Induction Motor, and a Proposal for a Vector Controlled Two-phase Induction Motor as a Replacement. *IEEE Trans Power Electron*. 2013; 28(1): 526-536.

[4] T Sutikno. The Preliminary Research for Implementation of Improved DTC Scheme of High Performance PMSM Drives. *TELKOMNIKA Telecommunication Computing Electronics and Control*. 2008; 6(3): 155-166.

[5] M Jannati, NRN Idris, Z Salam. *A New Method for Modeling and Vector Control of Unbalanced Induction Motors*. IEEE Energy Conversion Congress and Exposition. 2012; 3625-3632.

[6] M Jannati, A Monadi, NRN Idris, MJA Aziz, AAM Faudzi. Vector Control of Faulty Three-Phase Induction Motor with an Adaptive Sliding Mode Control. *Prz Elektrotech*. 2013; 89(12): 116-120.

[7] S Lekhchine, T Bahi, Y Soufi. Indirect rotor field oriented control based on fuzzy logic controlled double star induction machine. *Int J Electr Power Energy Syst*. 2014; 57: 206-211.

[8] P Vas P. Sensorless vector and direct torque control. Oxford University Press. 1998.

[9] P Castaldi P, W Geri, M Montanari, A Tilli. A new adaptive approach for on-line parameter and state estimation of induction motors. *Control Eng Practice*. 2005; 13(1): 81-94.

[10] K Akatsu, A Kawamura. On-line rotor resistance estimation using the transient state under the speed sensorless control of induction motor. *IEEE Trans Power Electron*. 2000; 15(3): 553-560.

[11] R Marino, S Peresada, CM Verrelli. Adaptive control for speed sensorless induction motors with uncertain load torque and rotor resistance. *Int J Adapt Control Signal Process*. 2005; 19(9): 661-685.

[12] O Aydogmus, S Sünter. Implementation of EKF based sensorless drive system using vector controlled PMSM fed by a matrix converter. *Int J Electr Power Energy Syst*. 2012; 43(1): 736-743.

[13] M Barut M, S Bogosyan, M Gokasan. Speed-sensorless estimation for induction motors using extended Kalman filters. *IEEE Trans Indust Electron*. 2007; 54(1): 272-280.

[14] EG Shehata. Speed sensorless torque control of an IPMSM drive with online stator resistance estimation using reduced order EKF. *Int J Electr Power Energy Syst*. 2013; 47: 378-386.

[15] A Lebaroud, A Medoued. Online computational tools dedicated to the detection of induction machine faults. *Int J Electr Power Energy Syst*. 2013; 44(1): 752-757.

[16] A Gaeta, G Scelba, A Consoli. Modeling and Control of Three-Phase PMSMs Under Open-Phase Fault. *IEEE Trans Indust Appl*. 2013; 49(1): 74-83.

[17] BL Rajalakshmi Samaga, KP Vittal. Comprehensive study of mixed eccentricity fault diagnosis in induction motors using signature analysis. *Int J Electr Power Energy Syst*. 2012; 35(1): 180-185.

[18] DR Espinoza-Trejo, DU Campos-Delgado, G Bossio, E Bárcenas, JE Hernández-Díez, LF Lugo-Cordero. Fault diagnosis scheme for open-circuit faults in field-oriented control induction motor drives. *IET Power Electron*. 2013; 6(5): 869-877.

[19] B Karanayil, MF Rahman, C Grantham. Online stator and rotor resistance estimation scheme using artificial neural networks for vector controlled speed sensorless induction motor drive. *IEEE Trans Indust Electron*. 2007; 54(1): 167-176.

[20] FR Salmasi, TA Najafabadi. An adaptive observer with online rotor and stator resistance estimation for induction motors with one phase current sensor. *IEEE Trans Energy Convers*. 2011; 26(3): 959-966.

[21] G Kenne, RS Simo, F Lamnabhi-Lagarrigue, A Arzande, JC Vannier. An online simplified rotor resistance estimator for induction motors. *IEEE Trans Control Syst Technol*. 2010; 18(5): 1188-1194.

[22] M Jannati, NRN Idris, MJA Aziz. *A new method for RFOC of Induction Motor under open-phase fault*. In Industrial Electronics Society, IECON. 2013; 2530-2535.

[23] M Jannati, E Fallah. *Modeling and Vector Control of Unbalanced induction motors (faulty three phase or single phase induction motors)*. 1st. Conference on Power Electronic & Drive Systems & Technologies (PEDSTC). 2010; 208-211.

[24] M Jannati, SA Anbaran, IM Alsofyani, NRN Idris, MJA Aziz. *Modeling and RFOC of Faulty Three-Phase IM Using Extended Kalman Filter for Rotor Speed* Estimation. 8th International Power Engineering and Optimization Conference (PEOCO2014). 2014; 270-275.

[25] M Jannati, E Fallah. *A New Method for Speed Sensorless Vector Control of Single-Phase Induction Motor Using Extended Kalman Filter*. Conf. Proc. Of ICEE. 2011; 1-5.

[26] M Jannati, A Monadi, NRN Idris, MJA Aziz. Speed Sensorless Vector Control of Unbalanced Three-Phase Induction Motor with Adaptive Sliding Mode Control. *International Journal of Power Electronics and Drive Systems (IJPEDS)*. 2014; 4(3): 406-418.

[27] M Jannati, A Monadi, SA Anbaran, NRN Idris, MJA Aziz. An Exact Model for Rotor Field-Oriented Control of Single-Phase Induction Motors. *TELKOMNIKA Indonesian Journal of Electrical Engineering*. 2014; 12(7): 5110-5120.

[28] M Jannati, SH Asgari, NRN Idris, MJA Aziz. Speed Sensorless Direct Rotor Field-Oriented Control of Single-Phase Induction Motor Using Extended Kalman Filter. *International Journal of Power Electronics and Drive Systems (IJPEDS)*. 2014; 4(4).

[29] M Jannati, NRN Idris, MJA Aziz, A Monadi, AAM Faudzi. A Novel Scheme for Reduction of Torque and Speed Ripple in Rotor Field Oriented Control of Single Phase Induction Motor Based on Rotational Transformations. *Research Journal of Applied Sciences, Engineering and Technology*. 2014; 7(16): 3405-3409.

Appendix A:
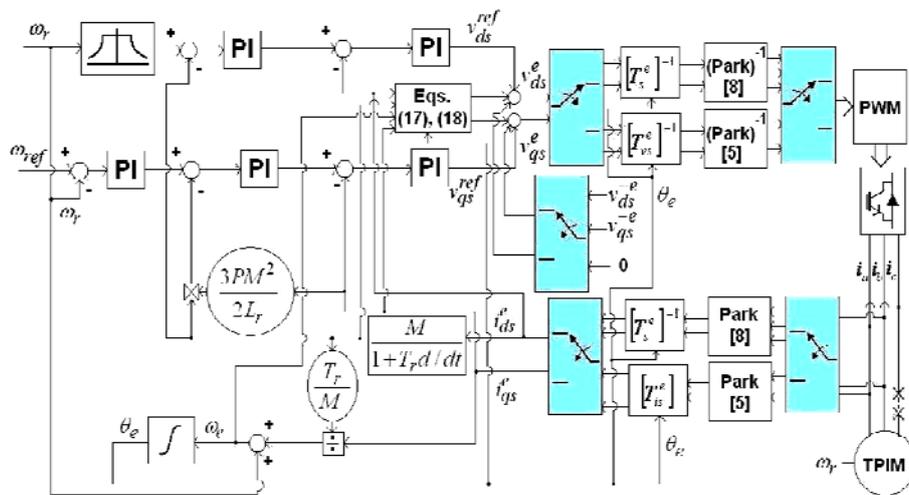
Fault-tolerant drive system based on IRFOC [5]

In the balanced mode we have: r_s, $M=3/2L_{ms}$ and $L_s=L_{ls}+3/2L_{ms}$

In the faulty mode we have: $r_s=(r_sM_q{}^2+r_sM_d{}^2)/2M_d{}^2$, $M=M_q=\sqrt{3}/2L_{ms}$ and $L_s=L_{qs}=L_{ls}+1/2L_{ms}$

Moreover: $\left[T_s^e\right]=\begin{bmatrix} \cos\theta_e & \sin\theta_e \\ -\sin\theta_e & \cos\theta_e \end{bmatrix}$

Appendix B:

Equation (1)-(8), which are used to model the FTPIM, can be written in the form following equation:

$$\begin{bmatrix} pi_{ds}^s \\ pi_{qs}^s \\ pi_{dr}^s \\ pi_{qr}^s \end{bmatrix} = \begin{bmatrix} -\xi_1 r_s L_r & \xi_1 \omega_r M_d M_q & \xi_1 M_d r_r & \xi_1 \omega_r M_d L_r \\ -\xi_2 \omega_r M_d M_q & -\xi_2 r_s L_r & -\xi_2 \omega_r M_q L_r & \xi_2 M_q r_r \\ \xi_1 r_s L_r M_d & -\xi_1 \omega_r M_q L_{ds} & -\xi_1 L_{ds} r_r & -\xi_1 \omega_r L_{ds} L_r \\ \xi_2 \omega_r M_d L_{qs} & \xi_2 r_s M_q & \xi_1 \omega_r L_{qs} L_r & -\xi_1 L_{qs} r_r \end{bmatrix} \begin{bmatrix} i_{ds}^s \\ i_{qs}^s \\ i_{dr}^s \\ i_{qr}^s \end{bmatrix}$$
$$+ \begin{bmatrix} \xi_1 L_r & 0 & -\xi_1 M_d & 0 \\ 0 & \xi_2 L_r & 0 & -\xi_2 M_q \\ -\xi_1 M_d & 0 & \xi_1 L_{ds} & 0 \\ 0 & -\xi_2 M_q & 0 & \xi_2 L_{qs} \end{bmatrix} \begin{bmatrix} v_{ds}^s \\ v_{qs}^s \\ 0 \\ 0 \end{bmatrix}$$

Where,

$$\xi_1 = \frac{1}{\sigma_1 L_{ds} L_r} \quad , \quad \xi_2 = \frac{1}{\sigma_2 L_{qs} L_r} \quad , \quad \sigma_1 = 1 - (\frac{M_d^2}{L_{ds} L_r}) \quad , \quad \sigma_2 = 1 - (\frac{M_q^2}{L_{qs} L_r})$$

Consequently, this equation can be written as follows:

$$\begin{bmatrix} p i_{dr}^s \\ p i_{qr}^s \\ p r_r \end{bmatrix} = \begin{bmatrix} -\xi_1 L_{ds} r_r & -\xi_1 \omega_r L_{ds} L_r & 0 \\ \xi_1 \omega_r L_{qs} r_r & -\xi_1 L_{qs} r_r & 0 \\ 0 & 0 & 1 \end{bmatrix} \begin{bmatrix} i_{dr}^s \\ i_{qr}^s \\ r_r \end{bmatrix} + \begin{bmatrix} \xi_1 r_s L_r M_d & -\xi_1 \omega_r M_q L_{ds} & -\xi_1 M_d & 0 \\ \xi_2 \omega_r M_d L_{qs} & \xi_2 r_s M_q & 0 & -\xi_2 M_q \\ 0 & 0 & 0 & 0 \end{bmatrix} \begin{bmatrix} i_{ds}^s \\ i_{qs}^s \\ v_{ds}^s \\ v_{qs}^s \end{bmatrix}$$

And,

$$\left(\begin{bmatrix} i_{ds}(n) \\ i_{qs}(n) \end{bmatrix} - \begin{bmatrix} 1 - \dfrac{r_{ds}}{\sigma_1 L_{ds}} dt & \dfrac{M_d M_q \omega_r}{\sigma_1 L_{ds} L_r} dt \\ -\dfrac{M_d M_q \omega_r}{\sigma_2 L_{qs} L_r} dt & 1 - \dfrac{r_{qs}}{\sigma_2 L_{qs}} dt \end{bmatrix} \begin{bmatrix} i_{ds}(n-1) \\ i_{qs}(n-1) \end{bmatrix} - \begin{bmatrix} \dfrac{v_{ds}^s}{\sigma_1 L_{ds}} dt \\ \dfrac{v_{qs}^s}{\sigma_2 L_{qs}} dt \end{bmatrix} \right) = \begin{bmatrix} \dfrac{M_d r_r(n)}{\sigma_1 L_{ds} L_r} dt & \dfrac{M_d \omega_r}{\sigma_1 L_{ds}} dt & 0 \\ -\dfrac{M_q \omega_r}{\sigma_2 L_{qs}} dt & \dfrac{M_q r_r(n)}{\sigma_2 L_{qs} L_r} dt & 0 \end{bmatrix} \begin{bmatrix} i_{dr}^s \\ i_{qr}^s \\ r_r \end{bmatrix}$$

So, matrices $A(n)$, $B(n)$ and $C(n)$ are obtained as follows:

$$A(n) = \begin{bmatrix} 1 - \dfrac{r_r(n)}{\sigma_1 L_r} dt & -\dfrac{\omega_r}{\sigma_1} dt & 0 \\ \dfrac{\omega_r}{\sigma_2} dt & 1 - \dfrac{r_r(n)}{\sigma_2 L_r} dt & 0 \\ 0 & 0 & 1 \end{bmatrix}$$

$$B(n) = \begin{bmatrix} \dfrac{M_d r_s}{\sigma_1 L_{ds} L_r} dt & -\dfrac{M_d \omega_r}{\sigma_1 L_r} dt & -\dfrac{M_d}{\sigma_1 L_{ds} L_r} dt & 0 \\ \dfrac{M_q \omega_r}{\sigma_2 L_r} dt & \dfrac{M_q r_s}{\sigma_2 L_{qs} L_r} dt & 0 & -\dfrac{M_q}{\sigma_2 L_{qs} L_r} dt \\ 0 & 0 & 0 & 0 \end{bmatrix}$$

$$C(n) = \begin{bmatrix} \dfrac{M_d r_r(n)}{\sigma_1 L_{ds} L_r} dt & \dfrac{M_d \omega_r}{\sigma_1 L_{ds}} dt & 0 \\ -\dfrac{M_q \omega_r}{\sigma_2 L_{qs}} dt & \dfrac{M_q r_r(n)}{\sigma_2 L_{qs} L_r} dt & 0 \end{bmatrix}$$

Appendix C:
        Ratings and parameters of simulated TPIM:

$v = 125V \quad , \quad f = 50HZ \quad , \quad P = 4 \quad , \quad r_s = 20.6\Omega \quad , \quad r_r = 19.15\Omega$

$L_{ls} = 0.0814 \quad , \quad L_{lr} = 0.0814H \quad , \quad L_{ms} = 0.851H \quad , \quad power = 475W$